JOURNAL OF COMPUTATIONAL PHYSICS **48**, 168–181 (1982)

Implicit Boundary Conditions for the Solution of the Parabolized Navier–Stokes Equations for Supersonic Flows*

M. BARNETT AND R. T. DAVIS

University of Cincinnati, Cincinnati, Ohio 45221

AND

J. V. RAKICH

NASA Ames Research Center, Moffett Field, California 94035

Received January 7, 1982

A fully implicit set of boundary conditions is developed for the solution of the parabolized Navier–Stokes equations for supersonic flow in two dimensions. Shock fitting is employed at the shock and the body has no-slip and specified temperature conditions. A specified heat transfer condition at the wall can be handled in a similar manner. In addition, the shock location is advanced in space in a fully implicit manner by utilizing the Rankine–Hugoniot conditions along with global conservation of mass.

INTRODUCTION

In [1] a parabolic form of the Navier–Stokes equations for supersonic compressible flow is solved using the Beam–Warming factored implicit algorithm [2]. External flows over bodies at angle of attack were calculated for the domain bounded by the body surface and the enveloping shock wave. In that work, and in most other works of a similar nature, the shock boundary conditions (the Rankine–Hugoniot jump conditions) are applied in an explicit manner. While adequate for small marching steps (within the CFL condition at the shock), the explicit method has a stability-imposed step size limitation. It is advantageous from the standpoint of computational efficiency to have fully implicit boundary conditions at both the shock and the body in order to remove this stability restriction on step size and allow the solution over a given domain to be obtained with less computational effort.

The earlier studies of Srivastava *et al.* [3] and Lubard and Helliwell [4] are examples of viscous shock layer calculations utilizing the Rankine–Hugoniot relations at the shock. The study of Srivastava *et al.* utilized a relaxation technique to obtain the overall solution and iterate on the shock shape. Lubard and Helliwell's study utilized space marching with iteration at each streamwise station. The solution scheme developed in the present study requires no iteration.

*This research was sponsored by NASA Ames Research Center under Contracts NCA2-OR130-901 and NCA2-OR130-101.

0021-9991/82/110168-14$02.00/0

Although the problem is viscous, the shock boundary condition can, for most applications, be treated in an inviscid manner, as viscous effects are mainly of interest near the solid boundary where a boundary layer exists. This implies that the Rankine–Hugoniot relations may be employed at the shock since the flow there is inviscid.

In the present study the equations are solved in block tridiagonal form by a matrix inverter tailored to solve four second-order equations. The set of equations which is solved here consists of two first-order and two second-order equations. To achieve compatibility with the inversion scheme, an appropriate finite difference scheme must be applied to the inviscid type equations at the boundaries. This situation is illustrated through a simple model problem. The use at the boundaries of a difference scheme such as that developed here removes what may be the source of oscillations in many numerical solution techniques. In the present parabolized Navier–Stokes solver, smooth solutions are obtained without the use of numerical smoothing schemes for flows without imbedded discontinuities.

Governing Equations and the Solution Scheme

The system of equations which is solved in this study is a parabolic form of the Navier–Stokes equations. The gas considered is laminar, perfect, and compressible.

The development of the basic solution scheme and the transformation from the physical to the computational plane follows much the same line of reasoning as was employed in [1].

Parabolization of the full Navier–Stokes equations is accomplished by assuming steady flow and neglecting streamwise diffusion in comparison to diffusion normal to the body surface. With these approximations, the governing equations can be written in nondimensional form as

$$\frac{\partial \bar{F}}{\partial \xi} + \frac{\partial \bar{G}}{\partial \eta} = \frac{\partial \bar{G}_v}{\partial \eta}. \tag{1}$$

These equations are in strong conservation form in the transform (ξ, η) plane where

$$\bar{F} = y_\eta F, \tag{2a}$$

$$\bar{G} = -y_\xi F + G, \tag{2b}$$

$$\bar{G}_v = -y_\xi F_v + G_v, \tag{2c}$$

with

$$F = \begin{bmatrix} \rho u \\ \rho u^2 + p \\ \rho uv \\ (\rho e_t + p)\, u \end{bmatrix}, \tag{2d}$$

$$G = \begin{bmatrix} \rho v \\ \rho uv \\ \rho v^2 + p \\ (\rho e_t + p)\, v \end{bmatrix}, \tag{2e}$$

$$F_v = \begin{bmatrix} 0 \\ \sigma_{xx} \\ \tau_{xy} \\ u\sigma_{xx} + v\tau_{xy} + q_x \end{bmatrix}, \tag{2f}$$

$$G_v = \begin{bmatrix} 0 \\ \tau_{xy} \\ \sigma_{yy} \\ u\tau_{xy} + v\sigma_{yy} + q_y \end{bmatrix}. \tag{2g}$$

The continuity, x momentum, y momentum, and energy equations are represented in each vector.

The above equations are written in the present case for the coordinate transformation defined by

$$x = \xi, \qquad y(\xi, \eta) = y_b(\xi) + s(\eta)\, \delta(\xi), \tag{3a), (3b)}$$

where $s(\eta)$ is the stretching function employed to cluster mesh points near the wall for proper boundary layer resolution and $\delta(\xi)$ is the shock standoff distance measured from body to shock along constant ξ. The corresponding Jacobian of the transformation is given by

$$J = 1/y_\eta = \eta_y. \tag{4}$$

The η coordinate is given by

$$\eta = (j - 1)\, \Delta\eta \tag{5a}$$

with $\eta = 0$ at the shock and $\eta = 1$ at the body. The index in the ξ direction is denoted by "i" so that

$$\xi = \xi_0 + i\Delta\xi \tag{5b}$$

with ξ_0 being the location of the initial data plane.

Typical physical and transformed planes and their nomenclature are given in Figs. 1a and b.

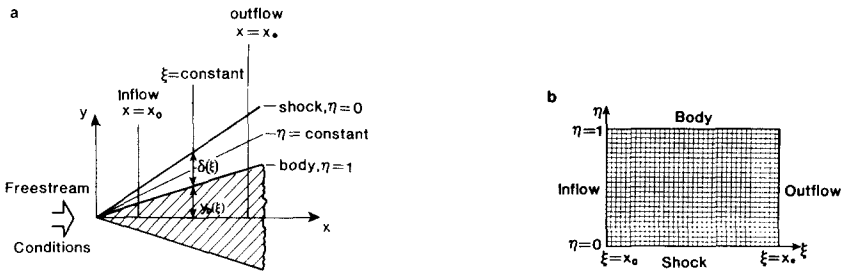

FIG. 1. (a) Typical physical plane geometry and notation; (b) typical computational plane.

The elements of F, G, F_v, and G_v can be written in terms of the elements of Q and their derivatives, where

$$Q = \begin{bmatrix} \rho \\ \rho u \\ \rho v \\ \rho e_t \end{bmatrix} \tag{6a}$$

and

$$\bar{Q} = Q/J. \tag{6b}$$

In the present formulation, the η momentum equation is assumed inviscid; this is a consistent assumption with regard to the order of magnitude of the terms already neglected as long as the body slope is small. The more appropriate assumption would be that the momentum equation for the direction normal to the body surface is inviscid.

The streamwise pressure gradient term is treated in a manner similar to that of [1] in order to prevent the appearance of departure solutions.

The development of the implicit finite difference scheme and appropriate linearization are discussed in detail in [5]. The finite difference scheme in incremental variable form is given by

$$\Delta^i \bar{F} + \Delta\xi \frac{\partial}{\partial \eta}(\Delta^i \bar{G} - \Delta^i \bar{G}_v) = \Delta\xi \frac{\partial}{\partial \eta}(-\bar{G}^i + \bar{G}_v^i), \tag{7}$$

where $\Delta^i z = z^{i+1} - z^i$ along $\eta = \text{const}$. Equation (7) is first-order accurate in ξ. Local linearization applied to (7) results in

$$\left[\frac{\partial \bar{F}}{\partial \bar{Q}} + \Delta\xi \frac{\partial}{\partial \eta}\left(\frac{\partial \bar{G}}{\partial \bar{Q}} - \frac{\partial \bar{G}_v}{\partial \bar{Q}}\right)\right]^i \Delta^i \bar{Q} = -\Delta\xi \frac{\partial}{\partial \eta}(\bar{G}^i - \bar{G}_v^i). \tag{8}$$

Discretization of Eq. (8) is performed later, after the boundary conditions have been developed.

Development of the Boundary Conditions

Equation (8) describes a sixth-order set of equations in the η direction, two first-order (continuity and η momentum), and two second-order (ξ momentum and energy) equations. Hence six boundary conditions are required and they must be distributed between the shock boundary and wall boundary in an appropriate manner. For the present purposes, three boundary conditions are applied at each boundary.

Shock Boundary

The physical unknowns at the shock are the incremental variables given by

$$\Delta Q_s = \begin{bmatrix} \Delta\rho \\ \Delta\rho u \\ \Delta\rho v \\ \Delta\rho e_t \end{bmatrix}_s \tag{9}$$

which can be rewritten, utilizing the shock jump relations of [6], in the form

$$\Delta Q_s = \begin{bmatrix} c_1 \\ c_2 \\ c_3 \\ c_4 \end{bmatrix} \Delta p_s = \bar{C}\,\Delta p_s, \tag{10}$$

where c_1–c_4 are obtained by locally linearizing about the shock slope and corresponding values of the flow variables at the previous march station. Hence the c_i's are all known. They are given by

$$c_1 = [(\gamma+1)/2\sin^2\theta]\,\rho_s[1-\rho_s(\gamma-1)/(\gamma+1)], \tag{11a}$$

$$c_2 = c_1 u_s - \rho_s, \tag{11b}$$

$$c_3 = \rho_s[\cot\theta - [(\gamma+1)/4\sin^3\theta\cos\theta](1-u_s)] + c_1 v_s, \tag{11c}$$

$$c_4 = 1/(\gamma-1) + c_2 u_s + c_3 v_s - c_1 \tfrac{1}{2}(u^2+v^2)_s. \tag{11d}$$

The jump conditions providing the above relationships are derived from conservation of mass, momentum, and energy at the shock. Through linearization they serve to reduce the four unknowns at the shock to one unknown parameter, Δp_s, hence providing three boundary conditions. The linearization performed here is consistent with the basic solution method, Eq. (8).

Because the strongly conservative form of the governing equations is used, an expression for $\Delta^i\bar{Q}$ is required, where

$$\bar{Q} = Q/J \qquad \text{and} \qquad \Delta^i\bar{Q} = (\Delta^i Q/J) - \bar{Q}^i(\Delta^i J/J^i). \tag{12}$$

In order to have a fully implicit method, the term $\Delta^i J$ in Eq. (12) must be evaluated in terms of the solution vector $\Delta^i \bar{Q}$. This is accomplished in the following manner: Based on the definitions of the Jacobian J and $y(\xi, \eta)$,

$$J = 1/\delta(\xi)\, s(\eta). \tag{13a}$$

Therefore, since ΔJ is taken along constant η, it follows that

$$\Delta^i J/J^i = -\Delta^i \delta/\delta^i. \tag{13b}$$

An implicit means for finding $\Delta^i \delta$ can be developed through the principle of global mass conservation. For this purpose the continuity equation is utilized in the form of Eq. (7). Thus,

$$\Delta^i \bar{f} + \Delta\xi \frac{\partial \Delta^i \bar{g}}{\partial \eta} = -\Delta\xi \frac{\partial \bar{g}^i}{\partial \eta}. \tag{14}$$

For the continuity equation, the appropriate variables are

$$\bar{f} = y_\eta \rho u = \overline{\rho u}, \tag{15a}$$

$$\bar{g} = -y_\xi \rho u + \rho v = -(y_\xi/y_\eta)\, \overline{\rho u} + (1/y_\eta)\, \overline{\rho v}. \tag{15b}$$

Equation (14) is next discretized across a box centered at $i + \frac{1}{2}, j - \frac{1}{2}$ to obtain

$$\tfrac{1}{2}(\Delta^i \bar{f}_j + \Delta^i \bar{f}_{j-1}) + (\Delta\xi/\Delta\eta)(\Delta^i \bar{g}_j - \Delta^i \bar{g}_{j-1}) = -(\Delta\xi/\Delta\eta)(\bar{g}^i_j - \bar{g}^i_{j-1}). \tag{16a}$$

Equation (16a) is now summed from shock to body, which is effectively trapezoidal rule integration, giving

$$\sum_{j=2}^{NJ} \frac{1}{2}(\Delta^i \bar{f}_j + \Delta^i \bar{f}_{j-1})\, \Delta\eta + \frac{\Delta\xi}{\Delta\eta} \sum_{j=2}^{NJ} (\Delta^i \bar{g}_j - \Delta^i \bar{g}_{j-1})\, \Delta\eta$$

$$= -\frac{\Delta\xi}{\Delta\eta} \sum_{j=2}^{NJ} (\bar{g}^i_j - \bar{g}^i_{j-1})\, \Delta\eta, \tag{16b}$$

where $j = NJ$ at the body. This is the appropriate integration for the present scheme. Performing the indicated summation and imposing the no-slip condition at the body results in

$$\tfrac{1}{2}(\Delta^i \bar{f}_1 + 2\Delta^i \bar{f}_2 + \cdots + 2\Delta^i \bar{f}_{NJ-1}) - (\Delta\xi/\Delta\eta)\, \Delta^i \bar{g}_1 = (\Delta\xi/\Delta\eta)\, \bar{g}^i_1. \tag{17}$$

The first term on the left-hand side of Eq. (17) is $-\Delta^i y_s$, the change in shock position between i and $i+1$, as next shown. Integrating the mass flux through the inflow and outflow planes of two subsequent ξ stations and setting the difference equal to the amount of mass admitted through the shock between those two stations (if no mass is injected at the body) leads to

$$\Delta^i y_s = -\int_0^1 \Delta^i(\rho u y_\eta)\, d\eta. \tag{18}$$

The right-hand side of Eq. (18) is the negative of the first term on the left-hand side of Eq. (17), giving

$$\Delta^i y_s = -(\Delta\xi/\Delta\eta)(\Delta^i \bar{g}_1 + \bar{g}_1^i). \tag{19}$$

Now since

$$y_s = y_b + \delta, \tag{20a}$$

it follows that

$$\Delta^i \delta = \Delta^i y_s - \Delta^i y_b. \tag{20b}$$

Equation (19) is then substituted into Eq. (20b) giving us an expression for $\Delta^i\delta$ in terms of the prescribed $\Delta^i y_b$, known terms, and the unknown $\Delta^i \bar{g}_1$ of continuity. Using this expression for $\Delta^i\delta$ together with Eq. (10) in Eq. (12) gives us the desired expression for $\Delta^i \bar{Q}_s$ in terms of one unknown parameter, $\Delta^i p_s$. Performing the above described manipulations and rearranging terms to solve for $\Delta^i \bar{Q}_s$ we can write in compact notation

$$\Delta\bar{Q}_s = \bar{S}(\Delta^i p_s/J^i) + \bar{T}, \tag{21}$$

where $\bar{S}$ and $\bar{T}$ are easily obtained.

Before proceeding to application of the boundary conditions at the shock using the finite difference scheme, we next turn to the body boundary conditions.

Wall Boundary

At the body the no-slip conditions ($u = v = 0$) are applied and the wall temperature is specified. This provides three boundary conditions.

We can write

$$\Delta Q_b = \begin{bmatrix} \Delta\rho \\ 0 \\ 0 \\ \Delta(\rho e_t) \end{bmatrix}_b \tag{22}$$

Since at the wall $e = e_t$, the equation of state yields

$$(\rho e_t)_b = e_w \rho_b, \tag{23a}$$

thus

$$\Delta(\rho e_t)_b = e_w \Delta\rho_b, \tag{23b}$$

where e_w is a constant given by

$$e_w = T_w/\gamma(\gamma - 1)\, M_\infty^2. \tag{23c}$$

Therefore we can write

$$\Delta Q_b = \begin{bmatrix} 1 \\ 0 \\ 0 \\ e_w \end{bmatrix} \Delta \rho_b. \tag{24}$$

We wish now to consider the form of $\Delta \bar{Q}_b$. According to Eq. (12) we can write

$$\Delta \bar{\rho} = (\Delta \rho / J) - \bar{\rho}(\Delta J / J), \tag{25a}$$

$$\Delta \overline{\rho e}_t = (\Delta \rho e_t / J) - \overline{\rho e}_t (\Delta J / J). \tag{25b}$$

Use of Eqs. (23a) and (23b) permits us to write

$$\Delta (\rho e_t)_b = e_w \Delta \bar{\rho}_b. \tag{26}$$

Finally we can write at the wall

$$\Delta \bar{Q}_b = \begin{bmatrix} 1 \\ 0 \\ 0 \\ e_w \end{bmatrix} \Delta \bar{\rho}_b. \tag{27}$$

As at the shock, one unknown parameter remains at the wall, $\Delta \bar{\rho}_b$.

Development of the Boundary Point Difference Scheme

The boundary conditions and use of the continuity equation has allowed us to express the eight unknowns at the shock and wall boundaries in terms of two unknowns, $\Delta^i p_s$ and $\Delta^i \bar{\rho}_b$, respectively. With application of a suitable finite difference scheme at the boundaries, the system of equations can be cast into block tridiagonal form, which results in a set of equations that is relatively easy to solve with existing methods, see [7], for example. We intend to show that there exists one particularly suitable finite difference scheme to use at the boundaries. Further, if the boundary point difference scheme can be developed directly from the interior point difference scheme, then the finite differencing will be completely compatible over the entire solution field. It will be demonstrated that incompatibility of the boundary point differencing with the interior point differencing can lead to oscillatory solutions.

Model Problem

A simple model problem is used to illustrate the above claims. It is desired to numerically integrate the equation

$$df/dy = \pi \cos \pi y, \qquad f(0) = 0, \tag{28}$$

over the interval $0 \leqslant y \leqslant 1$.

One might discretize Eq. (28) as

$$(f_{i+1} - f_i)/\Delta y = (\pi/2)(\cos \pi y_{i+1} + \cos \pi y_i). \tag{29a}$$

With a boundary condition on f at $i = 1$ ($f_1 = F$), the solution can be obtained at all points by stepping Eq. (29a) out from the boundary. If Eq. (29a) is written across $i - \frac{1}{2}$ by decrementing i by one and these two expressions are added together, one obtains the central difference form for constant Δy

$$(f_{i+1} - f_{i-1})/2\Delta y = (\pi/4)(\cos \pi y_{i+1} + 2 \cos \pi y_i + \cos \pi y_{i-1}). \tag{29b}$$

With Eq. (29b) the system of equations can be cast into tridiagonal form and solved by conventional methods using a tridiagonal inverter. This is how the model problem is solved in this study.

An alternative method of solution is the following: By stepping Eq. (29b) from $i = 1$, the solution can be obtained at all of the odd numbered mesh points. To obtain the solution at the even numbered mesh points, a difference expression relating f at i and $i + 1$ must be employed. The obvious choice is Eq. (29a) which can be employed once, and then, with the solution at one even numbered mesh point, Eq. (29b) can be marched backwards to find the solution at all remaining even numbered mesh points. This technique will give precisely the same solution as when Eq. (29a) is used for all points or when system (29b) is solved in tridiagonal form, as one would solve a second-order equation using (29a) as an outer boundary condition. Equation (29a) is not the only possible finite difference expression which can be used as an outer boundary condition or to transfer the solution to an even numbered mesh point when using Eq. (29b). It is, however, the only *compatible* difference expression for this task, having been used to derive the interior point difference scheme. This model problem was solved for this study using a tridiagonal inverter and the percent error in the solution is plotted for the compatible and an incompatible boundary point difference expression in which the derivative is written as a three-point backward difference at the upper boundary. Identical results are obtained using the odd and even point marching scheme mentioned above. The incompatible expression was not chosen at random. It has formally the same order of accuracy at the boundary point as the interior point difference scheme for df/dy has at those points. The results (Fig. 2) show that the incompatible boundary point differencing yields an oscillatory solution which reproduces the compatible differencing results only at the odd numbered mesh points. The solution has not been properly transferred to the even numbered mesh points.

If the solution method for this model problem utilizing Eqs. (29b) and (29a) is written out in matrix form, it is found to be a tridiagonal system with all zero elements on the main diagonal except at the upper boundary where Eq. (29a) is applied. This system is clearly lacking diagonal dominance, yet we note that this poses no problem provided the boundary point differencing is treated properly.

The situation can be summarized as follows: A first-order equation is integrated using a two-point central difference written across three mesh points. In order to

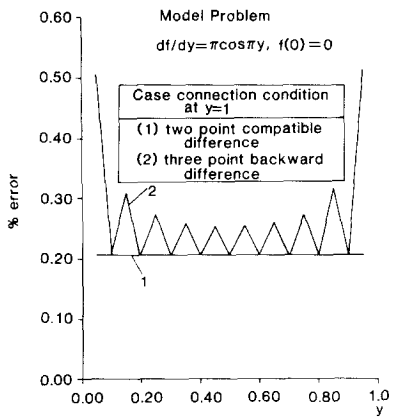

FIG. 2. Model problem: present error versus y at interior points.

correctly recouple the solution points, a "numerical boundary condition" is required which we shall call a "connection condition." Hence the first-order equation with a two-point central difference written across three mesh points requires one boundary condition and one connection condition. This is exactly analogous to the parabolic Navier–Stokes problem, which we recall was formulated with two inviscid equations.

We now proceed to develop the finite difference scheme for the solution of Eq. (8). Only the inviscid form of that equation is considered because the connection conditions are required only for the inviscid (first-order) equations.

Equation (8) is discretized across the box centered at $i+\frac{1}{2}, j+\frac{1}{2}$ for an inviscid equation as

$$\left[\frac{1}{2}\left(\frac{\partial \bar{f}}{\partial \bar{Q}}\bigg|_{j+1}+\frac{\partial \bar{f}}{\partial \bar{Q}}\bigg|_{j}\right)+\frac{\Delta\xi}{\Delta\eta}\left(\frac{\partial \bar{g}}{\partial \bar{Q}}\bigg|_{j+1}-\frac{\partial \bar{g}}{\partial \bar{Q}}\bigg|_{j}\right)\right]^{i}\Delta^{i}\bar{Q}$$
$$=-\frac{\Delta\xi}{\Delta\eta}(\bar{g}_{j+1}-\bar{g}_{j})^{i}. \tag{30}$$

As for the model problem, decrement j by one to give the expression for the box centered at $i+\frac{1}{2}, j-\frac{1}{2}$, then add this and Eq. (30) to give

$$\left[\frac{1}{4}\left(\frac{\partial \bar{f}}{\partial \bar{Q}}\bigg|_{j+1}+2\frac{\partial \bar{f}}{\partial \bar{Q}}\bigg|_{j}+\frac{\partial \bar{f}}{\partial \bar{Q}}\bigg|_{j-1}\right)+\frac{\Delta\xi}{2\Delta\eta}\left(\frac{\partial \bar{g}}{\partial \bar{Q}}\bigg|_{j+1}-\frac{\partial \bar{g}}{\partial \bar{Q}}\bigg|_{j-1}\right)\right]^{i}\Delta^{i}\bar{Q}$$
$$=-\frac{\Delta\xi}{2\Delta\eta}(\bar{g}_{j+1}-\bar{g}_{j-1})^{i}. \tag{31}$$

This is the interior point difference scheme for the inviscid terms in all of the conservation equations. Note that as for the model problem, the η derivatives are two-point central differences written across three mesh points. We should thus expect the same uncoupling of adjacent solution points in the inviscid equations as was

observed in the model problem. This also occurs in the viscous equations in inviscid regions where the viscous terms die out. Hence we choose to employ Eq. (30) at the two boundaries on the inviscid equations, one at each boundary. This will allow us to apply the correct connection conditions while at the same time providing a relationship between the one remaining unknown at each boundary and the solution vector at the adjacent mesh point. Thus the boundary points are eliminated from the inversion of the system of equations and the desired block tridiagonal form is achieved. Note that the present algorithm could be used for computing totally inviscid flows by providing two more required connection conditions.

The application of the connection conditions for the viscous problem is detailed in the next section.

Application of Connection Conditions

The continuity equation written in the form of Eq. (30) is utilized at the shock boundary. Using compact notation the equation is rewritten as

$$A\Delta^i\bar{Q}_1 + B\Delta^i\bar{Q}_2 = R. \tag{32a}$$

Noting that $\Delta\bar{Q}_s = \Delta\bar{Q}_1$, Eq. (21) is substituted into Eq. (32a) and $\Delta p_s/J$ solved for to yield

$$\Delta^i p_s/J^i = (A\bar{S})^{-1}[R - A\bar{T} - B\Delta^i\bar{Q}_2], \tag{32b}$$

expressing $\Delta p_s/J$ in terms of the unknown vector $\Delta\bar{Q}_2$ and known quantities. Next substituting Eq. (32b) into Eq. (21) gives $\Delta\bar{Q}_1$ in terms of $\Delta\bar{Q}_2$ and known quantities. The final step is to substitute for $\Delta\bar{Q}_1$ in terms of $\Delta\bar{Q}_2$ in the overall finite difference scheme written at $j = 2$ for all of the governing equations. This redefines the coefficient matrices and right-hand side term for $j = 2$ and eliminates the shock point from the direct inversion of the system of equations. Once $\Delta\bar{Q}_2$ is known, $\Delta\bar{Q}_1$ is obtained from the expression relating the two.

The procedure at the body is almost identical to that at the shock; therefore it will not be detailed here. The main difference is that at the body the connection condition is made on the η momentum equation.

The boundary conditions in conjunction with the connection conditions have been developed in this study in a completely implicit manner. One other point must be discussed, namely, the method for advancing the shock shape in a fully implicit manner.

Implicit Advance of the Shock Shape

Some parabolized Navier–Stokes schemes which employ shock fitting have in the past not used implicit means to advance the shock shape, even though the rest of the scheme may have been implicit. In [1] the authors note that the use of Euler explicit integration to march the shock shape downstream leads to restrictions on the

maximum allowable streamwise step size. It is found that an implicit method for advancing the shock can be developed straightforwardly based on global conservation of mass.

In [3], the shock shape is solved for implicitly by making the shock standoff one of the unknowns solved for when the equations are inverted. This is more costly than the present approach in terms of the computational effort required.

The integration indicated in Eq. (18) is all that is needed to implicitly advance the shock. Once the equations have been inverted at station $i+1$, the vector $\Delta^i \bar{Q}$ is known, hence $\Delta^i(\rho u y_\eta)$ is available. The integration of Eq. (18) is performed using the trapezoidal rule to find $\Delta^i y_s$. Then $\Delta^i \delta$ follows from Eq. (20b) with the prescribed $\Delta^i y_b$. Finally

$$\delta^{i+1} = \delta^i + \Delta^i \delta. \tag{33}$$

Once δ^{i+1} is known, J^{i+1} is computed and $\bar{Q}^{i+1}$ is decoded to give Q^{i+1}, the physical variables.

RESULTS

In this study a fully implicit set of boundary conditions for the parabolized Navier–Stokes equations in strong conservation form has been developed. Figure 3 shows the surface pressure for the 10% parabolic arc airfoil at the conditions solved for in an earlier numerical study by Schiff and Steger [8]. Agreement is good between the present code and their results. All profiles were found to be free of oscillations except for very small magnitude oscillations near the shock. No smoothing of any sort was applied in the present scheme.

The three-dimensional solution scheme of [1] was reduced to two dimensions and a step size study performed to compare the effect of the difference in the boundary conditions between the two schemes. The earlier scheme was found to be limited in step size to a condition which corresponds approximately to a CFL number of one at

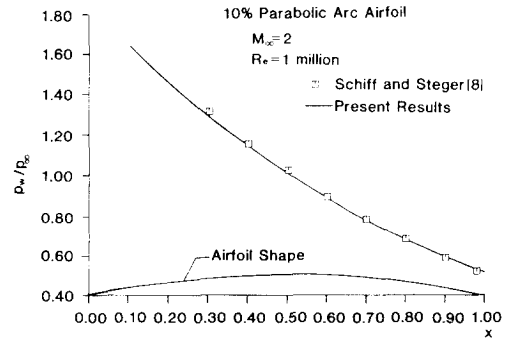

FIG. 3. Ten percent parabolic arc airfoil, ρ_w/ρ_∞ versus x.

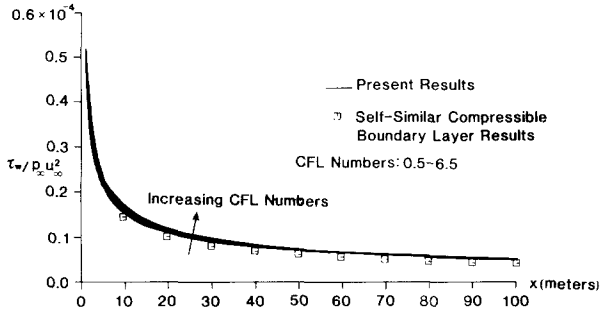

FIG. 4. Wall shear versus x for various CFL numbers for flat plate flow.

the shock. The present scheme permits shock CFL numbers up to approximately seven, although the accuracy of the results declines as expected at the higher CFL numbers. This is illustrated in Fig. 4 where wall shear profiles are plotted for various shock CFL numbers and are compared to the results of self-similar compressible boundary layer theory.

CONCLUSIONS

The importance of a carefully considered choice of the boundary point difference scheme has been indicated through a simple model problem. An implicit method has been devised for advancing the shock based on the principle of global mass conservation. It was found that if the present scheme is used with the shock advanced by Euler explicit integration, the maximum step size is again curtailed to a shock CFL number of approximately one, independent of the fact that the boundary conditions are otherwise fully implicit.

Though the present analysis is for two-dimensional flow, extension of the boundary conditions to three dimensions should be possible using the same principles.

APPENDIX: NOMENCLATURE

c_1, c_2, c_3, c_4	constants arising from linearized shock relations
e	specific internal energy
F, G	vectors in governing equations
i	index in streamwise (ξ) direction
j	index in stream-normal (η) direction
J	Jacobian of the coordinate transformation
M	Mach number
p	pressure
Q	vector of flow variables
u	velocity component in x-direction

v	velocity component in y-direction
x, y	Cartesian coordinates, physical plane
γ	ratio of specific heats, $\gamma = c_p/c_v$
δ	shock standoff distance
ξ, η	coordinates in transform plane
ρ	density

Subscripts

b	body
s	shock
t	total
v	viscous
w	wall
x, y	partial derivatives with respect to x and y, respectively
ξ, η	partial derivatives with respect to ξ and η, respectively
∞	freestream value

REFERENCES

1. Y. C. VIGNERON, J. V. RAKICH, AND J. C. TANNEHILL, "Calculation of Supersonic Viscous Flow over Delta Wings with Sharp Subsonic Leading Edges," AIAA Paper 78-1137, Seattle, Washington, July 1978.
2. R. F. WARMING AND R. M. BEAM, *SIAM–AMS Proc.*, **11**, 85.
3. B. N. SRIVASTAVA, M. J. WERLE, AND R. T. DAVIS, *AIAA J.* **16** (2)(1980), 137.
4. S. C. LUBARD AND W. S. HELLIWELL, *AIAA J.* **12** (7) (1974), 965.
5. M. BARNETT, "Solution of the Parabolized Navier–Stokes Equations by a Fully Implicit Method for Supersonic Flows with an Analysis of Departure Solution Behavior," M.S. Thesis, Dept. of Aerospace Engrg. and Appl. Mech., Univ. of Cincinnati, Ohio, August 1981.
6. "Equations, Tables, and Charts for Compressible Flow," NACA Report 1135, 1953.
7. J. L. STEGER, "Implicit Finite Difference Simulation of Flow about Arbitrary Geometries with Application to Airfoils," AIAA Paper 77-665, Albuquerque, New Mexico, June 1977.
8. L. B. SCHIFF AND J. L. STEGER, *AIAA J.* **18** (12) (1980), 1421.